Int. Journal of Refractory Metals and Hard Materials 42 (2014) 51–56

Contents lists available at ScienceDirect

Int. Journal of Refractory Metals and Hard Materials

journal homepage: www.elsevier.com/locate/IJRMHM

Sintering behavior of W–30Cu composite powder prepared by electroless plating

Lai-Ma Luo [a,c,*], Xiao-Yue Tan [a], Ze-Long Lu [a], Xiao-Yong Zhu [a,c], Xiang Zan [a,c], Guang-Nan Luo [b], Yu-Cheng Wu [a,c,*]

[a] College of Material Science and Engineering, Hefei University of Technology, Hefei 230009, China
[b] Institute of Plasma Physics, Chinese Academic Sciences, Hefei 230031, China
[c] Engineering Research Center of Powder Metallurgy of Anhui Province, Hefei 230009, China

ARTICLE INFO

Article history:
Received 13 July 2013
Accepted 17 October 2013

Keywords:
Electroless plating
W–Cu composite
Sintering behavior

ABSTRACT

Powder metallurgy technique was employed to prepare W–30 wt.% Cu composite through a chemical procedure. This includes powder pre-treatment followed by deposition of electroless Cu plating on the surface of the pre-treated W powder. The composite powder and W–30Cu composite were characterized by X-ray diffraction (XRD) and field emission scanning electron microscopy (FE-SEM). Cold compaction was carried out under pressures ranging from 200 MPa to 600 MPa while sintering at 850 °C, 1000 °C and 1200 °C. The relative density, hardness, compressive strength, and electrical conductivity of the sintered samples were investigated. The results show that the relative sintered density of the titled composites increased with the sintering temperature. However, in solid sintering, the relative density increased with pressure. At 1200 °C and 400 MPa, the liquid-sintered specimen exhibited optimum performance, with the relative density reaching as high as 95.04% and superior electrical conductivity of IACS 53.24%, which doubles the national average of 26.77%. The FE-SEM microstructure evaluation of the sintered compacts showed homogenous dispersion of Cu and W and a Cu network all over the structure.

1. Introduction

The properties of W–Cu composites, which are a combination of the high temperature strength of W and high thermal and electrical conductivities of Cu, make them appropriate candidates in a wide range of applications [1–3]. These materials can be used as arcing resistant electrodes, heavy-duty electronic contacts, heat sinks in high power microelectronic devices, welding electrodes for electro discharge machining, and divertor plates for fusion reactors [4,5]. The general method used for the fabrication of W–Cu composites is the infiltration of Cu into W skeleton. However, a homogeneous organizational structure with high weight percentage of W is hard to achieve in this process because of the difficulty in obtaining a uniform, porous W skeleton. The liquid-phase sintering of mixed powders is widely applied to fabricate the W–Cu composites. Unfortunately, W–Cu system exhibits mutual insolubility or negligible solubility, poor wettability, and high contact angle, such that its compacts show very poor sintering ability. Therefore, the fabrication of W–Cu composites with high relative densities and homogeneous microstructure is difficult [6–8]. In order to increase the wettability or decrease the contact angle of Cu and W for achieving full density, activators, such as Ni, Fe, and Co, have been used as the sintering aids for W–Cu composites. The challenge with this approach is that the sintering aids results in the deterioration of electrical and thermal conductivities of the composite materials [7–11]. The preparation of ultrafine nanosized particles by mechanical alloying [12,13] and activated sintering has been developed to improve the sintering strength and homogeneity of W–Cu composites. However, the mechanical alloying impurities, such as Fe and Co are introduced into the composites during severe milling from milling jar (stainless) and balls (cemented carbide or stainless). This also decreases the thermal and electrical conductivities of W–Cu composites. In recent years, a number of coating processes, such as electroless Ni [14,15] and Ni–P [16] plating have been developed essentially to address the above-mentioned drawbacks and improve the wettability of powder particles. The electroless Ni plating of metallic powders enhances composite homogeneity degree during pressing/sintering/infiltration. In this study therefore, W–30Cu composite powders were prepared by electroless plating and the W–30Cu composite obtained by conventional powder metallurgy method. The microstructure of the W–30Cu composites was observed by FESEM. The mechanical properties and electrical conductivity of the composites at different sintering conditions were also investigated.

2. Experimental

The W powder with Fisher particle size of 3 μm was activated by chemical activation pre-treatment. The surface of the activated W powder has some catalytic activity that is beneficial for coating with Cu by electroless plating. Activated W powders were put into

* Corresponding authors at: College of Materials Science and Engineering, Hefei University of Technology, Hefei 230009, China. Tel./fax: +86 551 62901012.
E-mail address: luolaima@126.com (L.-M. Luo).

0263-4368/$ – see front matter © 2013 Elsevier Ltd. All rights reserved.
http://dx.doi.org/10.1016/j.ijrmhm.2013.10.012

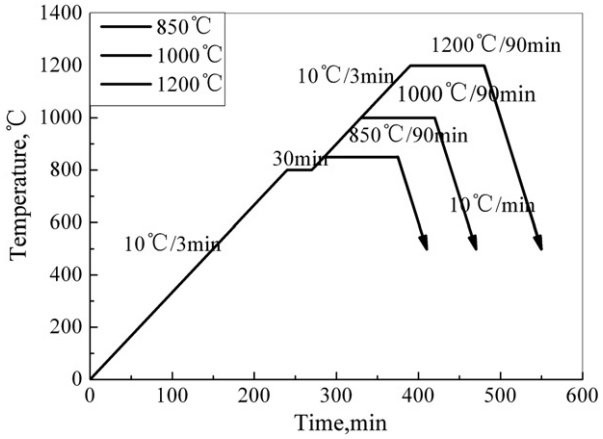

Fig. 1. Heating cycle for sintering.

the prepared Cu-plating solution for the electroless plating process. The plating solution consisted of copper sulfate, EDTA-2Na and 2,2′-bipyridine. During the electroless plating, the pH of the plating solution was adjusted from 11 to 13 with sodium hydroxide in order to control the rate of reaction. The amount of the copper sulfate in the plating solution was controlled to achieve about 30% Cu content for the W–Cu composite powders. The plating solution was continuously stirred to ensure a uniform dispersion of W powders during the reaction. The electroless plating was performed in a thermostat water bath at controlled temperature of 60 °C. After the electroless plating, W–30Cu composite powders were cleaned several times with de-ionized water until the residual liquid was clear. The composites were then dried in the oven at 50 °C. The prepared W–Cu composite powders were compacted into 32 × 8 mm dimension under various pressures of 200, 300, 400, 500, and 600 MPa.

The obtained green compacts were sintered in H_2 in a tubular sintering furnace at a heating rate of 10 °C/3 min. As depicted in Fig. 1, the samples were divided into three groups and subjected to sintering process at different temperature. The temperature of the first group was raised to 850 °C for 90 min for solid-phase sintering while those of the second and the third group were raised to 1000 °C, and 1200 °C respectively for 90 min, to conduct liquid-phase sintering. In order to facilitate solid phase sintering, the samples were first heated to 800 °C and kept at the temperature

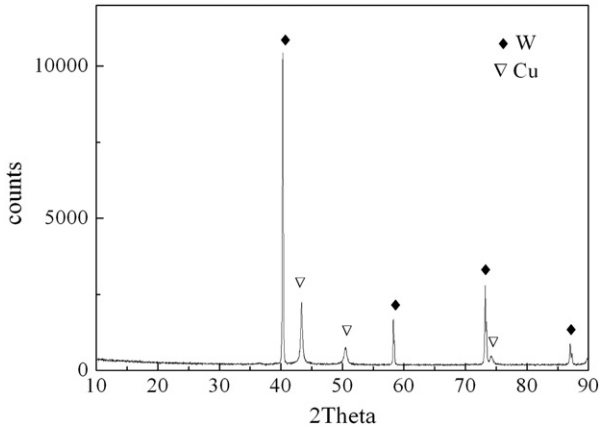

Fig. 2. XRD pattern of W–30Cu composite powder.

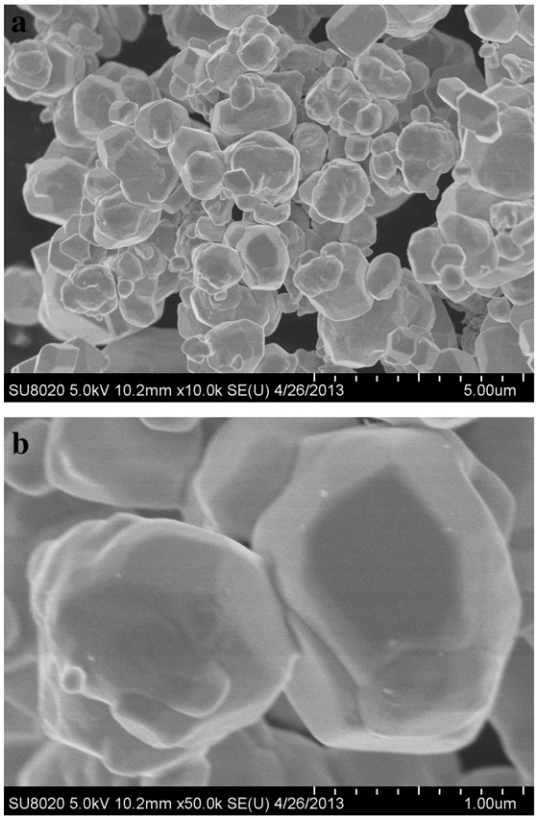

Fig. 3. FESEM photographs of the previous W powders.

for 30 min. This is necessary to exclude any moisture content and discharge any captured gases in the pores.

W–30Cu composite powder was characterized by XRD and FE-SEM. The relative density of the sintered W–30Cu composite was determined by Archimedes principle. FE-SEM was employed to observe the specimen's microstructure. Vickers micro-hardness was measured on polished sections as the average of 10 readings, using MH-3L micro-hardness tester along the cross-sectional surface of the specimen, with a load of 100 gf holding for 15 s. Compression test was performed using MTS-809 Axial/Torsional Test System machine and the electrical resistivity measured using a four-wire method.

3. Results and discussion

3.1. W–30Cu composite powder

The XRD pattern of the W–30Cu composite powder is displayed in Fig. 2. The pattern reveals the absence of other element's diffraction peaks, which indicates that the powders consist of W and Cu phases. Therefore, it can be concluded that the electroless plating did not introduce impurities into the W–30Cu composite powder.

Fig. 3 presents the FESEM micrographs of the original W before pre-treatment. As can be seen in the figure, the surface of the W particles is clean and smooth and has a polygonal structure. On the other hand, Fig. 4 illustrates the FESEM photographs after the electroless plating of the investigated W–Cu composite powders. Inspection of Fig. 4(a), with the higher magnification morphology shown in Fig. 4(b), indicates that almost no Cu uncoated-W particles were developed. Cu coatings on the surface

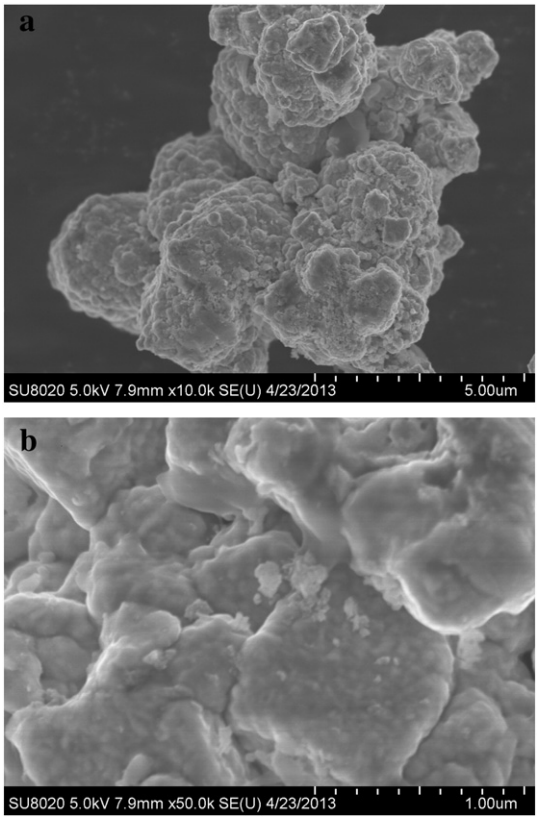

Fig. 4. FESEM photographs after the electroless plating of W–Cu composite powders.

of W particles showed a cell structure and have a dense, uniform distribution.

3.2. Green and sintered densities

Fig. 5 reveals the relative green and sintered densities as a function of compaction pressure after W–30Cu specimens have been sintered at 850, 1000, and 1200 °C for 90 min. Particularly, the sintered relative density of the specimens at 850 and 1000 °C, together with the relative green density increased with the compaction pressure. This may be attributed to the particle rearrangement, reduction in the pores sizes, and increase of the contact regions. The highest densification was obtained at pressure below 600 MPa owing to the expansion of contact between the particles, which resulted in the reduction of the pores between the particles. However, a significant densification of W–30Cu specimens occurred when compacted under 400 MPa and sintered at 1200 °C. This is important for the W–Cu liquid-phase sintering system, in that densification is predominated mainly by the particle rearrangement [8,17]. A compaction pressure above 400 MPa will lead to a decrease in the sintering density, even if the contact between the particles expands and the pores sizes reduce during compaction. This phenomenon is due to the condensation of W skeleton, which will usually obstruct particle rearrangement.

3.3. Microstructure characterization

Fig. 6(a)–(f) shows the metallographic microstructures of the significant densities of W–30Cu composites at different sintering temperature. It is obvious that the densification of the microstructure is consistent with the result displayed in Fig. 5. The FESEM morphologies of the fractured W–30Cu composites are as given in Fig. 7(a)–(f). As can be observed in the figures, W particles had no obvious growth and its previous polygonal structure, displayed in Fig. 3, becomes spherical. This must have been because Cu that surrounded W particle composite powders prevented the growth of these particles. A number of voids, indicated by arrows in Fig. 7(b), were found between the W particles, which lead to specimen's low density. This is a result of sintering at low temperature. Inter-granular fracture exists in the W–Cu composite, and the specimen showed some form of ductility. This generated some plastic deformation at the contacts between W with copper as indicated by arrows in Fig. 7(d)–(f). As evident in Fig. 7(f), some thin Cu layers existed as necks between W particles and formed Cu network all over the structure. The network improved the densification during sintering. Apparently, the Cu network structure may be attributed to electroless plating method used to obtain the composite powders.

3.4. Electrical conductivity

The measured electrical conductivity of the investigated composites is presented in Fig. 8. The imaginary line denotes the electrical conductivity of GB IACS 42%. As can be observed in the figure, W–30Cu composite has an excellent electrical conductivity at liquid sintering. On the whole, W–30Cu composite material has the highest density, structural homogeneity, Cu network structure, and the highest electrical conductivity. It also can be seen that the electrical conductivity increases with sintering temperature. This may be attributed to the fact that density is temperature dependent. The electrical conductivity reaches 53.24% at intermediate pressure with liquid-sintering, which is higher than the national standard of 26.77%. This is because the specimen has high density at 1200 °C and 400 MPa.

3.5. Hardness measurements

Relative density and mechanical behavior are directly related; the higher the density, the greater the hardness. The microstructural homogeneity can also be characterized by the quantitative analysis of the hardness values for the composites [18]. Vickers microhardness values of the investigated materials are presented in Fig. 9. For each specimen, the significant densities of the composites at different temperature are used in the plot. Each Vickers microhardness values produced some amplitude of variation, which may

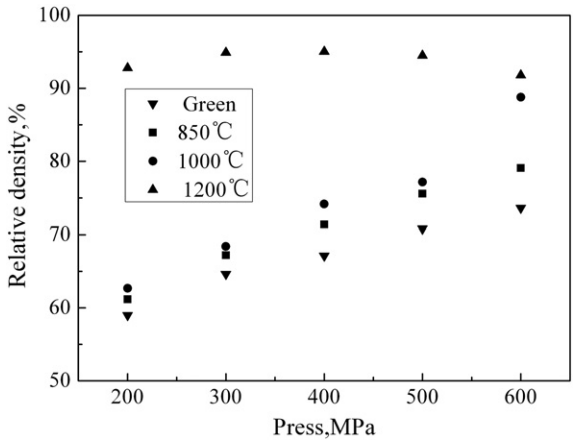

Fig. 5. Relative density of W–30Cu green and sintered composites versus compaction pressure.

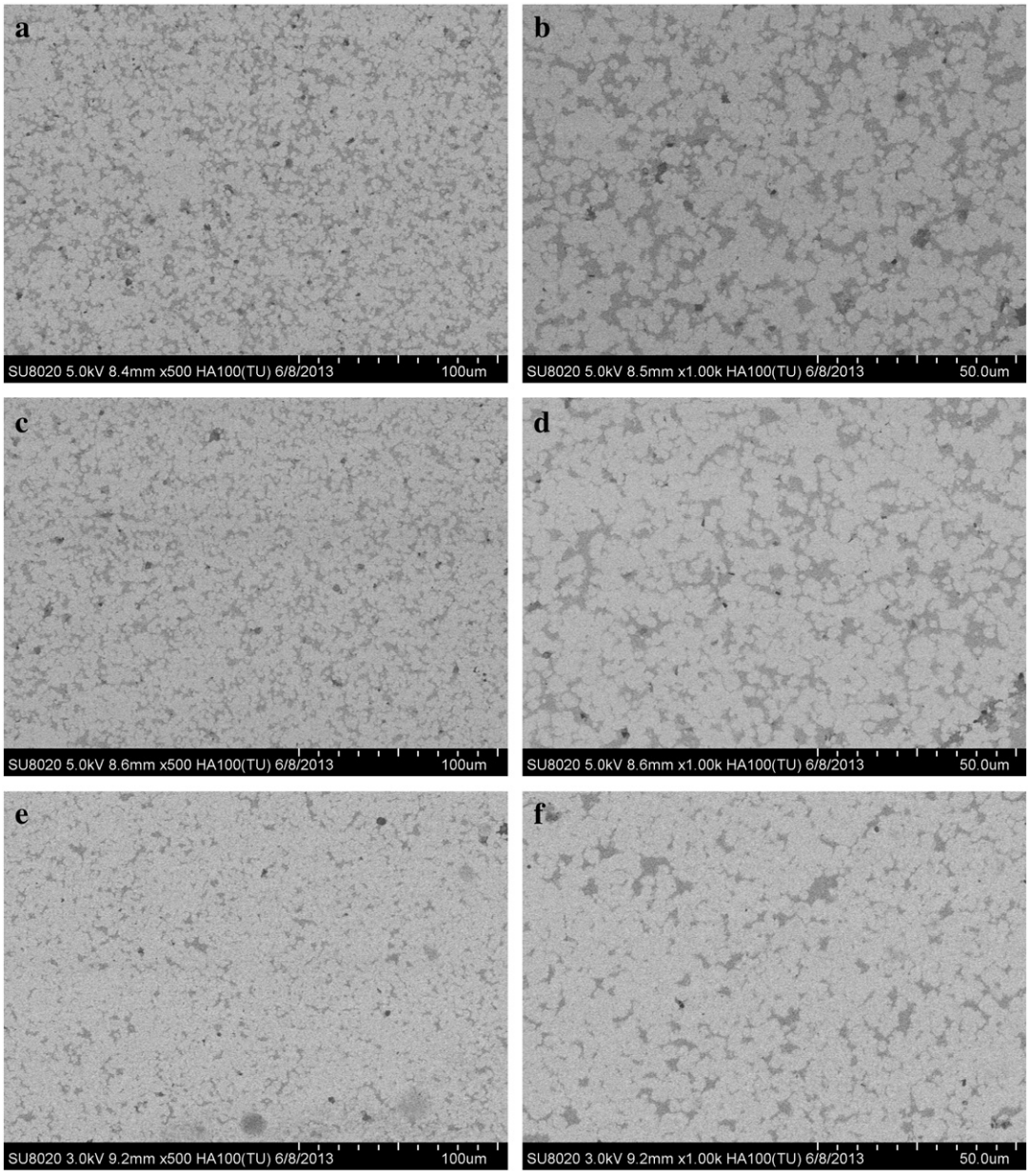

Fig. 6. SEM images of W–30Cu composite after sintered at respective process.(a)(b) 600 MPa, 850 °C; (c)(d) 600 MPa, 1000 °C; (e)(f) 400 MPa, 1200 °C.

be attributed to the microregion of Cu depleted from W particles. This region generated by the movement, erosion, and local agglomeration of W particles by liquid sintering is due to the hydrostatic forces as a result of the heterogeneities in the thermal flow of Cu melt. Nevertheless, the optimal value of the micro-hardness increased from 153.75 HV to 181.5 HV. This value indicates that the microstructure of the composite was very homogenized.

3.6. Compressive strength

Fig. 10 shows the room temperature compressive strength of W–30Cu composites. Porosity is considered as a suitable site for stress concentration, where crack nucleation and growth may take place. The compressive strength increased with the densification of W–30Cu samples; the higher the density, the less the porosity. The maximum compressive strength was 747.2 MPa.

4. Conclusions

This paper presents the electroless plating method, followed by powder metallurgy, to prepare W–30Cu composites. The following results were obtained:

1. SEM of W–30Cu composite powders showed Cu with a cell dense structure and uniform coating on the surface of W particles.
2. Dense W–30Cu composites can be obtained by electroless plating and powder metallurgy. With different sintering processes, the maximum relative density is 95.04% at 400 MPa compaction pressure and 1200 °C sintering.
3. Microstructure characterization reveals Cu network all over the structure of MW–30Cu composite; it has the highest electrical conductivity of 53.24%, which is greater than the national standard of 26.77%.

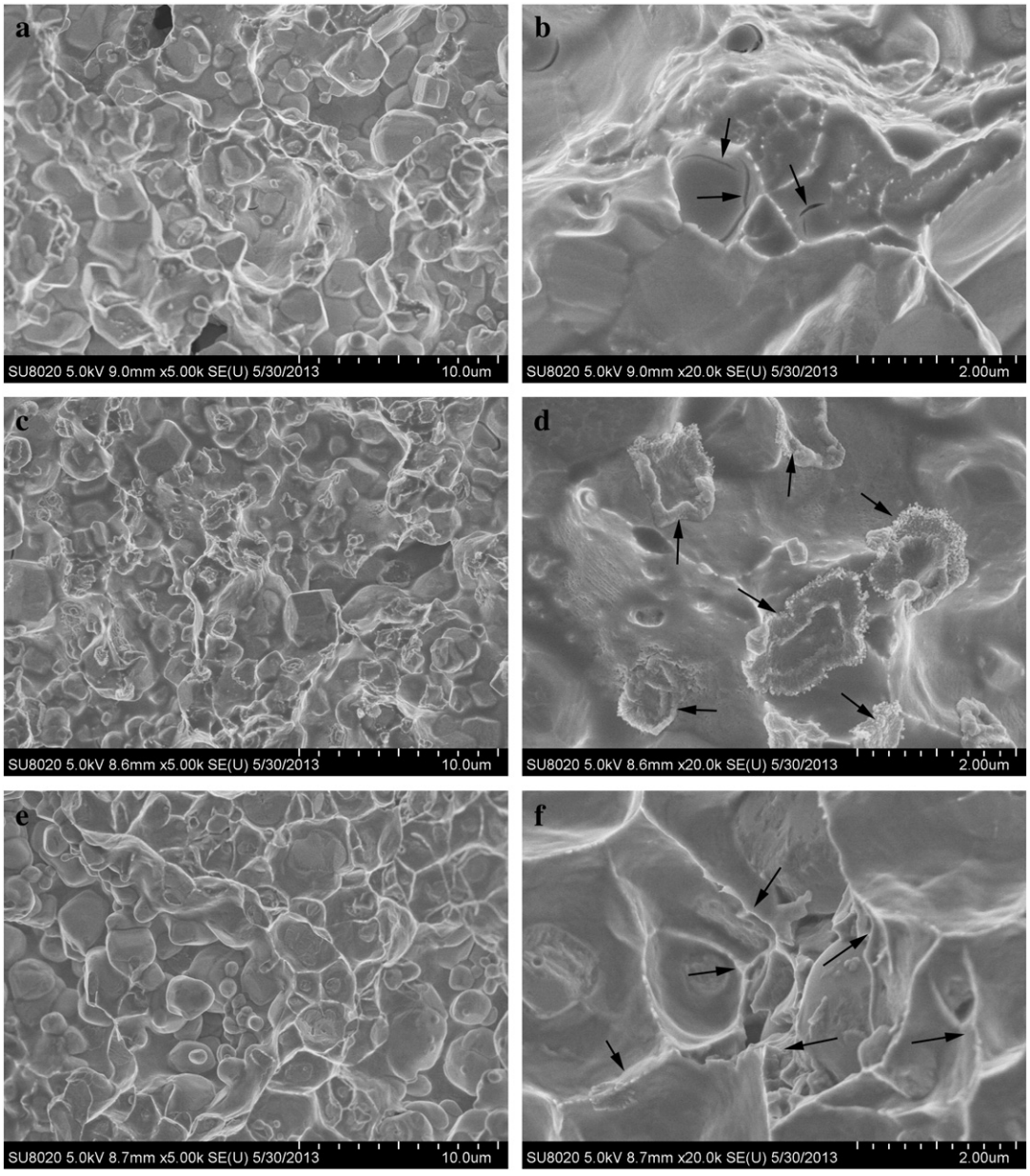

Fig. 7. Fractured SEM morphology of W–30Cu composites. (a)(b) 600 MPa, 850 °C; (c)(d) 600 MPa, 1000 °C; (e)(f) 400 MPa, 1200 °C.

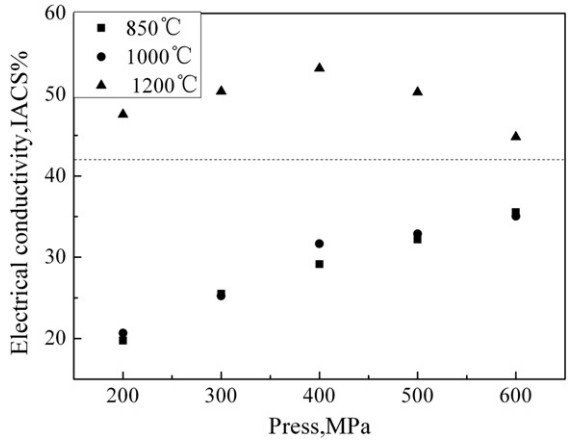

Fig. 8. Electrical resistivity of W–30Cu composites under different processes.

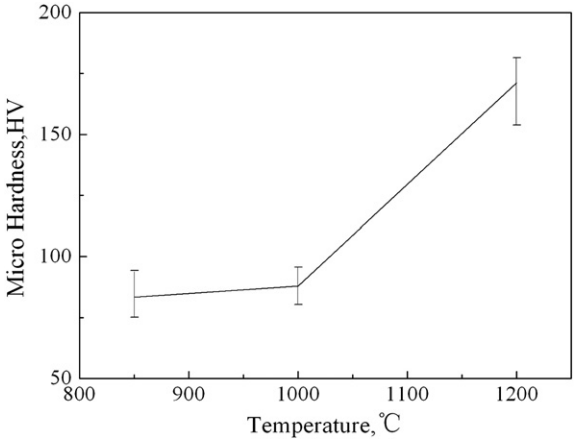

Fig. 9. Micro-hardness investigated for W–30Cu composites.

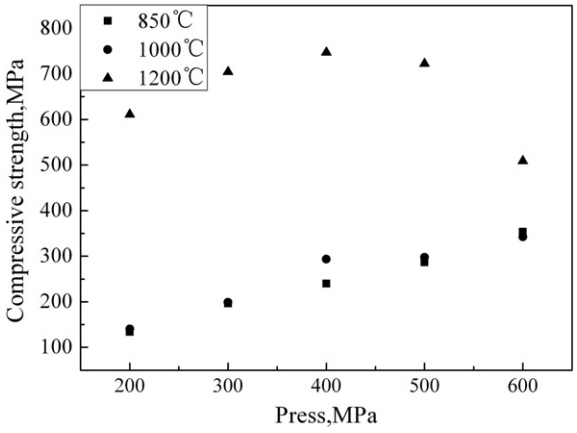

Fig. 10. Compressive strength investigated for W–30Cu composites.

Acknowledgment

This paper was supported by National Natural Science Foundation of China no. 51204064, and National Magnetic Confinement Fusion Program with Grant no. 2010GB109004.

References

[1] Wang CC, Lin YC. Feasibility study of electrical discharge machining for W/Cu composite. Int J Refract Met Hard Mater 2009;27:872–82.
[2] Abu-Oqail A, Ghanim M, El-Sheikh M, El-Nikhaily A. Effects of processing parameters of tungsten–copper composites. Int J Refract Met Hard Mater 2012;35:207–12.
[3] Ibrahim H, Aziz A, Rahmat A. Effects of cobalt addition and temperature on microstructure and density of W–25Cu composites prepared via liquid infiltration. Adv Mater Res 2012;626:430–5.
[4] Chen PG, Luo GQ, Li MJ, Shen Q, Zhang LM. Effects of Zn additions on the solid-state sintering of W–Cu composites. Mater Des 2012;36:108–12.
[5] Zhap P, Guo SB, Liu GH, Chen YX, Li JT. Fabrication of Cu-riched W–Cu composites by combustion synthesis and melt-infiltration in ultrahigh-gravity field. J Nucl Mater 2013;441:343–7.
[6] Gao JX, Li YG, Tian Y, Jiao Y. Ultrafine W–Cu composite powder research progress. Adv Mater Res 2012;535–537:86–9.
[7] Abbaszadeh H, Masoudi A, Safabinesh H, Takestani M. Investigation on the characteristics of micro- and nano-structured W–15 wt.% Cu composites prepared by powder metallurgy route. Int J Refract Met Hard Mater 2012;30:145–51.
[8] Ardestani M, Rezaie HR, Arabi H, Razavizadeh H. The effect of sintering temperature on densification of nanoscale dispersed W–20–40%wt Cu composite powders. Int J Refract Met Hard Mater 2009;27:862–7.
[9] Hong SH, Kim BK. Fabrication of W–20 wt.% Cu composite nanopowder and sintered alloy with high thermal conductivity. Mater Lett 2003;57:2761–7.
[10] Yoon ES, Lee JS, Oh ST, Kim BK. Microstructure and sintering behavior of W–Cu nanocomposite powder produced by thermo-chemical process. Int J Refract Met Hard Mater 2002;20:201–6.
[11] Özkal B, Upadhyaya A, Öveçoğlu, German RM. Comparative properties of 85W–15Cu powders prepared using mixing, milling and coating techniques. Powder Metall 2010;53:236–43.
[12] Maneshian MH, Simchi A. Solid state and liquid phase sintering of mechanically activated W–20 wt.% Cu powder mixture. J Alloys Compd 2008;463:153–9.
[13] Zhu YB, Shen YF, Gu DD, Wu P, Huang Z. Microstructural studies of W–Cu nanostructured precursor composite powders prepared by mechanical alloying. Powder Metall 2007;50:223–7.
[14] Peng XL. Preparation of nickel and copper coated fine tungsten powder. Mater Sci Eng A Struct 1999;262:1–8.
[15] Zangeneh-Madar K, Amirjan M, Parvin N. Improvement of physical properties of Cu-infiltrated W compacts via electroless nickel plating of primary tungsten powder. Surf Coat Technol 2009;203:2333–6.
[16] Amirjan M, Zangeneh-Madar K, Parvin N. Evaluation of microstructure and contiguity of W/Cu composites prepared by coated tungsten powders. Int J Refract Met Hard Mater 2009;27:729–33.
[17] Fan JL, Liu T, Zhu S, Han Y. Synthesis of ultrafine/nanocrystalline W–(30–50)Cu composite powders and microstructure characteristics of the sintered alloys. Int J Refract Met Hard Mater 2012;30:33–7.
[18] Kim DG, Kim GS, Suk MJ, Oh ST, Kim YD. Effect of heating rate on microstructural homogeneity of sintered W–15 wt.% Cu nanocomposite fabricated from W–CuO powder mixture. Scr Mater 2004;51:677–81.